Structural and Magnetic Properties of Multilayered TiO_2/FM/TiO_2/FM/$CoFe_2O_4$ (FM: Fe or Py) Films Grown by Pulsed Laser Deposition

Fabio D. Saccone[1], Paolo Vavassori[2,3], and Andreas Berger[2]

[1]Instituto de Tecnologias y Ciencias de la Ingenieria, INTECIN (UBA-CONICET), Buenos Aires C1063ACV, Argentina
[2]CIC NanoGUNE, Donostia-San Sebastian E-20018, Spain
[3]IKERBASQUE, The Basque Foundation for Science, Bilbao E-48011, Spain

Two types of multilayered thin films of structure TiO_2/FM/TiO_2/FM/$CoFe_2O_4$ with FM = Fe or Py were grown by means of the pulsed layer deposition technique with a total thickness of less than 350 nm. Their structural properties were analyzed by X-ray diffraction and the Fe K-edge absorption was measured by X-ray fluorescence in grazing incidence geometry. By means of near edge absorption X-ray spectroscopy (XANES), we retrieved information about the octahedral Fe^{+3} environment within the cobalt ferrite ($CoFe_2O_4$) films as well as the role of titanium oxide (TiO_2) as a good protective layer for these multilayered systems. The bulk magnetic properties of both samples exhibit certain similarities: at 10 K, the coercive field of their hysteresis loops is enhanced to approximately 1 T, with an intermediate magnetization drop occurring at approximately 2000 Oe reverse field strength, indicating the separated magnetization reversal behavior of pinned and unpinned grains within the FM layers. In contrast to this low temperature field dependence, the collective magnetic behavior is gradual upon field inversion when hysteresis loops are measured at or near room temperature. By using the FORC diagram technique at room temperature, we investigated this gradual transition in more detail and identified clear differences in between the two FM layer materials.

Index Terms—**Ferrite films, magnetic materials, magnetic superlattices.**

I. Introduction

DURING the last several years, Cobalt ferrite ($CoFe_2O_4$) films have been increasingly investigated by the scientific community because of their exceptionally attractive properties such as high coercivity and permeability at high frequencies, high chemical and mechanical stability for industrial purposes and relatively low conductivity. There is an increasing interest in magnetic ferrite nanoparticles and thin films because of their broad applications in several technological fields including permanent magnets, magnetic fluids, magnetic drug delivery, microwave devices, and high density information storage [1], [2]. The cobalt ferrite structure corresponds to the completely inverse spinel and the experimental magnetic moment, which is higher than expected for this structure and can be attributed to a contribution from an orbital magnetic moment that is incompletely quenched by the crystal field. Cobalt ferrite has an inverse spinel structure with A-sites (tetrahedral coordination of four O^{2-} ions) and B-sites (octahedral coordination of six O^{2-} ions). In the ideal inverse spinel, the A-sites must completely be occupied by Fe^{3+} ions and the B-sites must be randomly occupied by the remaining Fe^{3+} ions together with the Co^{2+} ions. However, Co-ferrite usually exhibits a mixed spinel structure, that is, an intermediate degree of inversion where both sites contain a fraction of Co^{2+} and Fe^{3+} cations. Furthermore, the occupation of tetrahedral sites by the divalent Co atoms depends on the preparation method [3].

It is widely known that the exchange-bias phenomenon induces shifts as well as coercive field increases in hysteresis loops of nanostructured magnetic materials composed of both antiferromagnetic (AFM) and ferromagnetic (FM) phases. The general observation of exchange bias in AFM/FM hybrid structures can also be applied to diluted ferrimagnets (fM), such as cobalt ferrite, for which defects or vacancies in the bulk are responsible for the net interlayer exchange coupling at the interface in between the fM and an adjacent ferromagnetic (FM) layer [4]. In this way, it is possible to induce a magnetic hardening of FM layers by field cooling of FM/fM hybrid structures. Even all ferromagnetic exchange bias systems, combining soft and hard magnetic layers, have been reported [5], [6]. It has been reported that exchange bias composite systems based on exchange coupling in between ferromagnetic (FM) and antiferromagnetic (AF) interfaces are very suitable as permanent magnets [7] and cobalt ferrite was successfully utilized as a pinning layer in spin valve devices [8]. In this paper, we added a soft FM layer to the FM/fm bilayer in order to study the coupling behavior of a soft (free FM layer) and a hard (pinned FM/fM bilayer) phase, like that present in exchange-spring magnetic systems.

One of the powerful techniques for film growth is pulsed laser deposition (PLD). It is especially useful due to its ability to preserve the target composition during film growth, which is particularly relevant for complex oxide or nitride materials.

The First Order Reversal Curve (FORC) diagram technique and associated methodologies are helpful tools in order to obtain information about irreversible switching fields of ferromagnetic structures including nanostructured materials. This technique consists of the measurements of a set of FORC curves. Each FORC curve starts initially at positive saturation field. The magnetic field is then reduced to a specific value (H_a), upon which the magnetic field is increased again until the saturating field is reached once more, while measuring the magnetization at all intermediate applied field values. This process is then repeated for different field values of the point, at which the field change is inverted.

Manuscript received February 15, 2013; revised March 27, 2013; accepted April 09, 2013. Date of current version July 23, 2013. Corresponding author: F. D. Saccone (e-mail: fabio.saccone@gmail.com).

Color versions of one or more of the figures in this paper are available online at http://ieeexplore.ieee.org.

Digital Object Identifier 10.1109/TMAG.2013.2258331

We apply the expression given by

$$\rho(H_a, H_b) = -\frac{\partial^2 M(H_a, H_b)}{\partial H_a \partial H_b} \quad (1)$$

to allow for a graphical representation of all FORC curves in a single diagram (see [10]). The diagram can also be described in terms of the mean and coercive fields of hysterons, by means of

$$h_c = \frac{1}{2}(H_b - H_a) \quad , h_u = \frac{1}{2}(H_a + H_b). \quad (2)$$

The axes corresponding to the reversion field (H_a) and inner field (H_b) are rotated 45° with respect to the mean hysteron field (h_u) and coercive hysteron field (h_c) axes, respectively [9].

FORC diagrams can provide a powerful tool for the classification and understanding of magnetization reversal that cannot be identified by simple hysteresis curve measurements. On a FORC diagram, each magnetic system exhibits a characteristic pattern, which contains detailed information about the magnetic reversal properties [10], [11]. In specific cases, such as perpendicular magnetic recording media, it is possible to determine even a single grain of information from the complex and collective magnetization reversal behavior by methods based on FORC data sets [12], [13].

II. Experimental Details

Iron (III) nitride nanohydride (Fe $(NO_3)_3.H_2O$, 99%, Anedra) and cobalt (II) chloride hexahydride ($CoCl_2.6\ H_2O$, 98%, Cicarelli) were used to synthesize $CoFe_2O_4$ nanoparticles by coprecipitation in a NaOH medium, keeping the molar ratio of Co/Fe $= 0.5$. For this process, each ingredient was dissolved in NaOH solution and then the solutions were mixed. The digestion was performed at 80 °C for 120 min. After digestion, the gelatinous precipitate was filtered and washed several times using deionized water until the pH value of the solution became neutral. Finally, the gelatinous precipitate was dried at room temperature in air to obtain a powder sample. Using the XRD technique in conjunction with grain size refinement following the Debye-Scherrer formula, the powder particle diameter d was determined to be 50 nm approximately. These nanoparticles of $CoFe_2O_4$ were used for powder compaction in order to fabricate a target, which was sintered subsequently. Commercial TiO_2 powder was used for preparing the corresponding target and pieces of iron and permalloy (Py) were employed as metallic targets for PLD.

Two single layer cobalt ferrite films (150 and 300 nm thick), multilayered TiO_2 (10 nm)/Fe(25 nm)/TiO_2(5 nm)/Fe(25 nm)/$CoFe_2O_4$(260 nm)/Si(100) (T_1 type) samples, and TiO_2 (10 nm)/Py(17.5 nm)/TiO_2 (5 nm)/Py(17.5 nm)/$CoFe_2O_4$ (260 nm)/Si(100) (T_2 type) samples were grown by the PLD technique using a Nd-YAG laser (quanta ray-spectra physics), a substrate temperature of 600 °C and a base pressure of 4×10^{-4} mbar. The target-substrate distance was 8 cm, and the repetition rate of the laser pulses was kept at 10 Hz, while using a fluence at the target surface of 2 J/cm^2. Under these conditions, the growth rate was measured to be approximately 10^{-2} nm per pulse. Grazing incidence XRD diffraction revealed a certain preferred orientation along the (440) direction for the cobalt ferrite films and allowed us to identify all crystallographic phases of the multilayered systems.

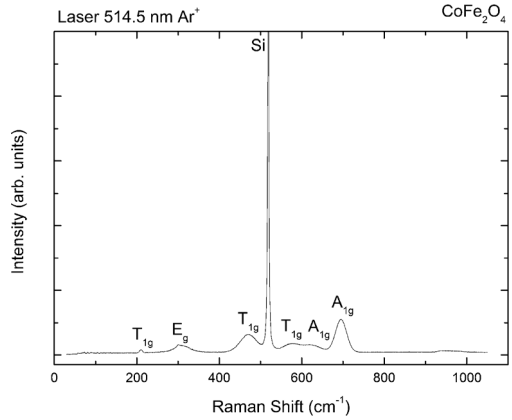

Fig. 1. Raman spectrum of a cobalt ferrite film grown by PLD. The vibrational modes corresponding to the inverse spinel are indicated as T_{1g}, A_{1g} and E_g.

Raman spectra were collected in the backscattering geometry using a 514.5 nm Ar laser and a Jobin-Yvon spectrometer in combination with a thermoelectric-cooled multichannel CCD detector with spectral resolution below 2 cm^{-1}. A laser power of less than 10 mW was used to avoid sample heating. Additional details on the Raman setup can be found elsewhere [14].

Room-temperature near edge X-ray-absorption fine structure (XANES) spectra at the Fe K edge were recorded in fluorescence mode using a Si(111) monochromator in the beamline of the LNLS (Campinas, Brazil).

Hysteresis loops and first order reversal curve (FORC) measurements were performed with a Quantum Design PPMS 9 T that was equipped with a VSM head option. For the assembly of the FORC diagrams, 50 FORC curves was measured.

III. Results and Discussion

A. Structural Characterization of Films and Multilayers

Fig. 1 shows the Raman spectra of one of our pure cobalt ferrite films. The most intense mode corresponds to the Si substrate, while six other modes can be clearly identified and are related to vibrational modes of the inverse spinel structure. The A_{1g} mode is related to the stretching of bonds between the A sites and the oxygen atoms. The nonsymmetrical splitting of the A1g vibrational mode (see the small maximum with a wave number of 630 cm^{-1} approximately) is an indication that the structure of the cobalt ferrite in the film corresponds to the inverse spinel, with a nonideal relative occupation [15].

XANES spectra corresponding to the Fe K-edge for single layer CoFe2O4 films grown with two different thicknesses (t $=$ 150 and 300 nm) can be seen in Fig. 2(a). The spectra were taken at an incidence angles above the total reflection condition, as described in the figure caption. The spectra exhibit the characteristics of a pure phase [16] with an absorption edge at 7121.9 eV, consistent with an oxidation state of 2.9 for Fe atoms, which is similar to that observed for samples prepared by the sol-gel method [17]. However, a small difference is present: for thinner

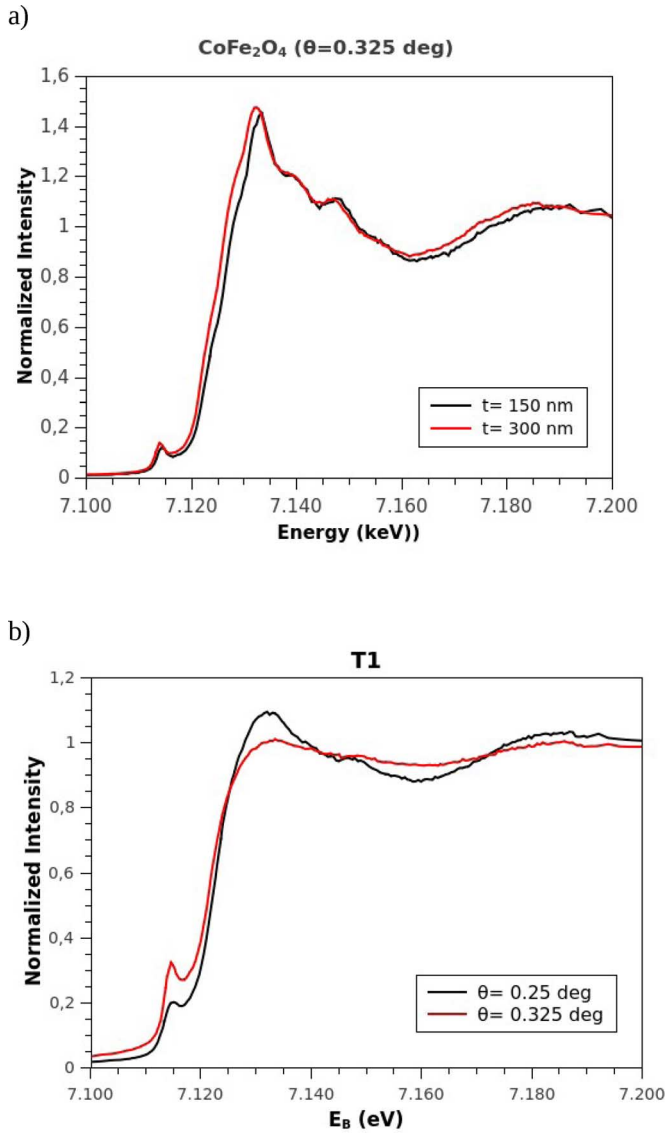

Fig. 2. (a) XANES spectrum of cobalt ferrite films (thickness of 150 and 300 nm). (b) XANES spectrum of multilayers T1 and T2.

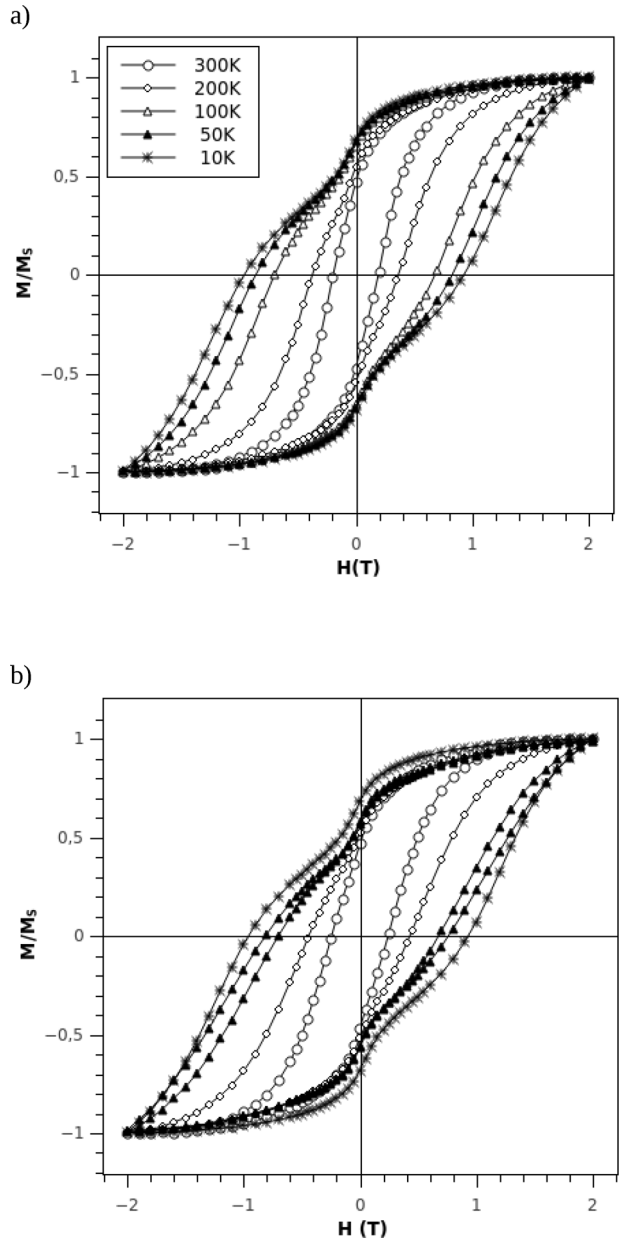

Fig. 3. (a) Magnetization as a function of applied field (measured at the temperatures indicated in the graph) for T1 sample after FC. (b) Magnetization as a function of applied field for T2 sample after FC [at the same temperatures indicated in (a)].

films, the edge energy and white line are slightly lower, which could indicate a more distorted environment for the octahedral Fe^{+3} sites [18].

The T1 XANES spectrum [Fig. 2(b)], corresponding to a smaller incident angle ($\theta = 0.25$ deg), exhibits a pattern that is more characteristic for Fe in an oxidized state than the spectrum corresponding to $\theta = 0.325$ deg, which shows more in-depth information. This last example has similar characteristics to that corresponding to an Fe foil (in particular, the white line has an amplitude with the same height than the corresponding to the second wave at 40 eV from the K-edge). When we are taking spectra at a deeper conditions, we get information from inner layers of our films (in our case, the external layer is TiO_2 and below this it grew a Fe layer). For T2 sample, the results are similar, and for this case it should be also mentioned that the Py films are more stable against oxidation than the Fe ones. Then, we can conclude from this fact that the TiO_2 layer acted as a good protective layer for both systems.

B. Magnetic Properties

Hysteresis loops of the multilayers were measured at different temperatures, after field cooling (FC) with an applied cooling field of 2 T [Fig. 3(a) and (b)]. At low temperature, they show characteristics such as those expected for "exchange-spring" magnets, when a decoupling between a hard and a soft phase exists. A significant magnetic hardening was observed for both samples after cooling in their respective remanent states and a bias field H_{EB} was determined at $T = 10$ K (-0.012 T for T1 and -0.018 T for T2). These behaviors originated from the interaction between the pinned Fe layer and the diluted fM ($CoFe_2O_4$). For both samples, the magnetization behavior below 200 K exhibits a drop to approximately half the saturation

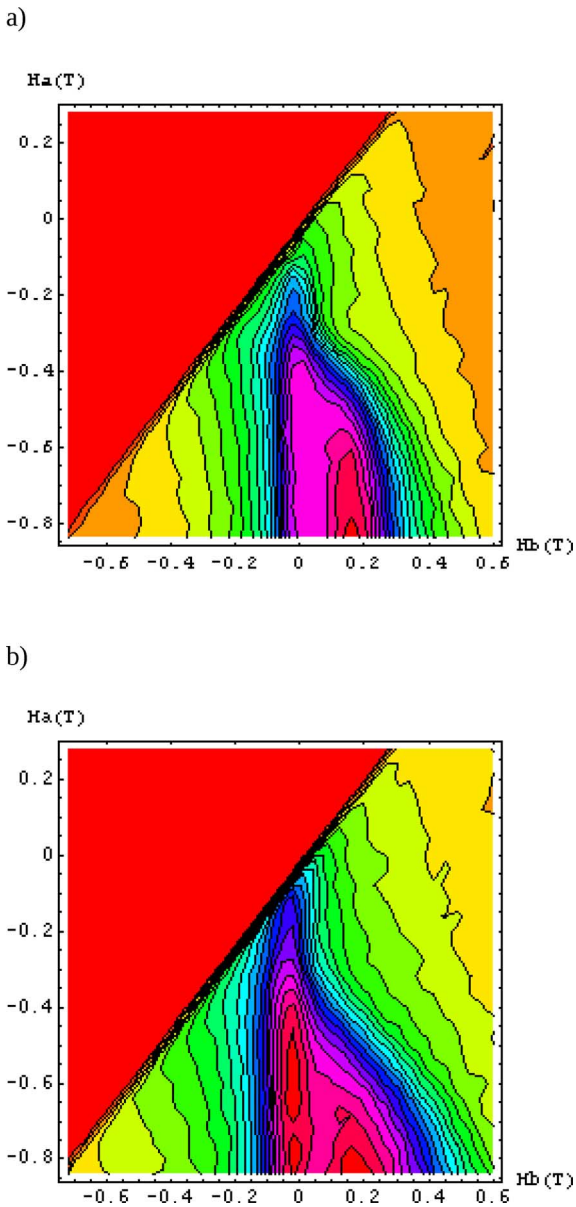

Fig. 4. (a) FORC diagram (at RT) of the T1 sample. (b) FORC diagram (at RT) of the T2 sample.

magnetization at around 2000 Oe reverse field, a value that is close to the coercive field of these samples at 300 K. This difference in the collective magnetization behavior can be attributed to the increase in coercive field experienced by the fM/FM set at low temperatures, while other regions of the multilayers have undergone magnetization reversal already at around 2000 Oe reverse field. Above 200 K, this differentiated collective magnetization behavior disappears. To elucidate this, we performed FORC curves measurements at room temperature (RT) and constructed their corresponding diagrams. These results can be observed in Fig. 4(a) and (b).

The line separating the uniform red background from the rest of the diagram is the h_u axis, i.e., $h_c = 0$ and thus separates reversible from irreversible magnetization processes. It can be seen in both figures that the hysteron populations have maximum structure that is elongated in the vertical direction or equivalently along -45° in the hu-hc plane. Both diagrams exhibit some similarities with FORC patterns that were observed for systems in which there is an interaction between a soft and a hard magnetic phase, such as the exchange-spring magnets [19], and it was found by Panagiotopoulos [20] that this interaction pushes the FORC distribution maxima of both phases along the directions parallel to the hu and hc axes. According to this FORC distribution analysis, certain conditions can cause an overlap between the hard and soft maximum, just as we find here for our samples.

Furthermore, it can be observed for the T2 sample [Fig. 4(b)], with its FM layers made from Py, that the FORC diagram exhibits two separated maxima at RT, corresponding to a more distributed collective magnetic behavior, in which some grains exhibit a very low coercive field. On the other hand, we found from the hysteresis loop that the Py containing samples exhibits a magnetic hardening at low temperature that is not gradual as in the T_1 sample, in which the magnetic films are made from Fe. It should be remarked that both samples have separating layers with the same thicknesses. Besides this, it was found there is better coupling between the Fe layer and the Fe/$CoFe_2O_4$ bilayer for the sample T1.

IV. Conclusion

We have grown by means of the pulsed laser deposition technique (PLD), multilayered magnetic materials systems, specifically: TiO_2 (10 nm)/Fe(25 nm)/TiO_2 (5 nm)/Fe(25 nm)/$CoFe_2O_4$ (260 nm)/Si(100) (T1 type sample) and TiO_2 (10 nm)/Py(17.5 nm)/TiO_2 (5 nm)/Py(17.5 nm)/$CoFe_2O_4$ (260 nm)/Si(100) (T2 type sample). For the $CoFe_2O_4$ target fabrication, we utilized nanoparticles synthesized by a chemical method. Through Raman and XANES spectroscopy, we demonstrated that the pure cobalt ferrite films grown by PLD with targets made by employing this nanoparticle process have indeed the partially inverted spinel structure. It was also observed that, for thinner films, the environment of the octahedral Fe^{+3} sites is more distorted. XANES spectra taken at grazing incidence allowed us to conclude that the TiO_2 acts as a good protective layer for the metallic ferromagnetic films in our structures.

From hysteresis loops measurements taken under ZFC conditions, we observed a magnetic hardening induced by the exchange bias phenomenon, which causes a separation of the magnetic response of the hardened grains from the soft ones. Analysis by means of the FORC diagram technique at RT allowed us to show that for the T1 sample (with Fe as free and pinned layer), the collective magnetic behavior is more homogeneous than in the case of the T2 structure (with Py as a free and pinned layer). For the T2 type sample, we also find a substantial hysteron population at low field in the corresponding FORC diagram, hereby identifying the existence of grains with lower coercivity.

Acknowledgment

This work was supported in part by the Brazilian Synchrotron Laboratory (Campinas, SP). The work of F. D. Saccone was supported by a grant from CONICET. Work at nanoGUNE was

supported by the Basque Government under the Etortek Program IE11-304 and Project PI2012-47 as well as the Spanish Ministry of Education under Project MAT2012-36844. The authors would also like thank to D. Errandonea (Valencia University) for the Raman spectroscopy measurements and discussion of the results.

REFERENCES

[1] G. Dascalu, D. Durneata, and O. F. Caltun, "Magnetic measurements of RE-Doped cobalt ferrite thin films," *IEEE Trans. Magn.*, vol. 49, no. 1, pp. 46–49, Jan. 2013.

[2] T. Sodaee, A. Ghasemi, E. Paimozd, A. Paesano, Jr., and A. Morisako, "The role of terbium cation substitution on the magnetic properties of cobalt ferrite nanoparticles," *J. Magn. Magn. Mater.*, vol. 330, pp. 169–173, Mar. 2013.

[3] R. A. McCurrie, *Ferromagnetic Materials (Structure and Poperties)*, 1st ed. London, U.K.: Academic, 1994, ch. 4.

[4] U. Nowak, K. D. Usadel, J. Keller, P. Miltenyi, B. Beschoten, and G. Guntherodt, "Domain state model for exchange bias. I. theory," *Phys. Rev. B*, vol. 66, p. 014430, Jul. 2002.

[5] A. Berger, D. T. Margulies, and H. Do, "Magnetic hysteresis loop tuning in antiferromagnetically coupled bilayer structures," *Appl. Phys. Lett.*, vol. 85, p. 1571, Aug. 2004.

[6] A. Berger, O. Hovorka, G. Friedman, and E. E. Fullerton, "Nonlinear and hysteretic exchange bias in antiferromagnetically coupled ferromagnetic bilayers," *Phys. Rev. B*, vol. 78, p. 224407, Dec. 2008.

[7] I. Betancourt and H. A. Davies, "Exchange coupled nanocomposite hard magnetic alloys," *Mater. Sc. Tech.*, vol. 26, pp. 5–19, Jan. 2010.

[8] M. Matsuda and H. Sakakima, "Magnetoresistance curves of spin valves using the (110) cobalt ferrite pinning layer," *J. Phys. D: App. Phys.*, vol. 44, p. 105001, 2011.

[9] F. Béron, D. Ménard, and A. Yelon, "Magnetic behavior of Ni/Cu multilayer nanowire arrays studied by first-order reversal curve diagrams," *IEEE Trans. Magn.*, vol. 44, no. 11, pp. 2745–2748, Nov. 2008.

[10] C. R. Pike, A. P. Roberts, and K. L. Verosub, "Characterizing interactions in fine magnetic particle systems using first order reversal curves," *J. Appl. Phys.*, vol. 85, pp. 6660–6667, May 1999.

[11] C. R. Pike, C. A. Ross, R. T. Scalettar, and G. Zimanyi, "First-order reversal curve diagram analysis of a perpendicular nickel nanopillar array," *Phys. Rev. B*, vol. 71, p. 134407, Apr. 2005.

[12] A. Berger, B. Lengsfield, and Y. Ikeda, "Determination of intrinsic switching field distributions in perpendicular recording media (invited)," *J. Appl. Phys.*, vol. 99, p. 08E705, 2006.

[13] O. Hovorka, Y. Liu, K. A. Dahmen, and A. Berger, "On the ability to determine intrinsic switching field distributions from hysteresis loops in the partially correlated magnetization reversal regime," *Appl. Phys. Lett.*, vol. 95, p. 192504, Feb. 2010.

[14] R. Lacomba-Perales, D. Errandonea, D. Martinez-Garcia, P. Rodríguez-Hernández, S. Radescu, A. Mujica, A. Muñoz, J. C. Chervin, and A. Polian, "Phase transitions in wolframite-type $CdWO_4$ at high pressure studied by Raman spectroscopy and density-functional theory," *Phys. Rev. B*, vol. 79, p. 094105, Mar. 2009.

[15] P. Chandramohan, M. P. Srinivasan, S. Velmurugan, and S. V. Narasimhan, "Cation distribution and particle size effect on Raman spectrum of $CoFe_2O_4$," *J. Solid State Chem.*, vol. 184, no. 1, pp. 89–96, Jan. 2011.

[16] D. Carta, G. Mountjoy, G. Navarra, M. F. Casula, D. Loche, S. Marras, and A. Corrias, "Magnetic and structural investigation of highly porous $CoFe_2O_4$-SiO_2 nanocomposite aerogels," *J. Phys. Chem. C*, vol. 111, p. 6308, Apr. 2007.

[17] R. S. Turtelli, M. Atif, N. Mehmood, F. Kubel, K. Biernacka, W. Linert, R. Grössinger, Cz. Kapusta, and M. Sikoram, "Interplay between the cation distribution and production methods in cobalt ferrite," *Mater. Chem. Phys.*, vol. 132, p. 832, Feb. 2012.

[18] C. E. Rodríguez Torres, F. Golmar, M. Ziese, P. Esquinazi, and S. P. Heluani, "Evidence of defect-induced ferromagnetism in $ZnFe_2O_4$ thin films," *Phys. Rev. B*, vol. 84, p. 064404, Aug. 2011.

[19] J. E. Davies, O. Hellwig, E. E. Fullerton, J. S. Jiang, S. D. Bader, G. T. Zimányi, and K. Liu, "Anisotropy dependence of irreversible switching in Fe/SmCo and FeNi/FePt exchange spring magnet films," *Appl. Phys. Lett.*, vol. 86, p. 262503, Jun. 2005.

[20] Panagiotopoulos, "A simple approach to the first order reversal curves (FORC) of two-phase magnetic systems," *J. Magn. Magn. Mat.*, vol. 323, p. 2148, Aug. 2011.